ORNL/TM-2024/3453

Preliminary Experimental Results in Support of the Development of EPP and SMT Design Methods and Viscoplastic Model for A709

Yanli Wang

July 2024

OAK RIDGE National Laboratory

ORNL IS MANAGED BY UT-BATTELLE LLC FOR THE US DEPARTMENT OF ENERGY

ORNL/TM-2024/3453

Materials Science and Technology Division

PRELIMINARY EXPERIMENTAL RESULTS IN SUPPORT OF THE DEVELOPMENT OF EPP AND SMT DESIGN METHODS AND VISCOPLASTIC MODEL FOR A709

Yanli Wang

July 2024

Prepared by
OAK RIDGE NATIONAL LABORATORY
Oak Ridge, TN 37831
managed by
UT-BATTELLE LLC
for the
US DEPARTMENT OF ENERGY
under contract DE-AC05-00OR22725

This page intentionally left blank.

CONTENTS

LIST OF FIGURES

LIST OF TABLES

ACKNOWLEDGMENTS

This research was sponsored by the United States (U.S.) Department of Energy (DOE) under Contract No. DE-AC05-00OR22725 with Oak Ridge National Laboratory (ORNL), which is managed and operated by the University of Tennessee– Battelle LLC. Programmatic direction was provided by the DOE Office of Nuclear Energy (NE).

The author gratefully acknowledges the support provided by Sue Lesica, Federal Materials Lead for the DOE-NE Advanced Reactor Technologies (ART) Program, Kaatrin Abbott, Federal Manager, DOE-NE ART Fast Reactor Program (FRP), and Bo Feng of Argonne National Laboratory, National Technical Director for DOE-NE's FRP.

The author extends thanks to ORNL staff members Bradley J Hall, C. Shane Hawkins and Jeremy Moser for their technical support in carrying out the experiments. The time spent by Lianshan Lin and Zhili Feng of ORNL reviewing this report is acknowledged.

Special thanks are extended to Ting-Leung Sham of the U.S. Nuclear Regulatory Commission (NRC), who served as the Advanced Materials Technology Area Lead for the ART Program within DOE-NE and supported this work prior to joining the US-NRC in FY2024.

ABSTRACT

The ASME code qualification effort for Alloy 709 (A709) is currently underway to qualify it for Class A construction in the American Society of Mechanical Engineers (ASME) Boiler and Pressure Vessel Code, Section III, Division 5. The United States (U.S.) Department of Energy (DOE) national laboratories are collaborating in the advanced materials development initiative to investigate the mechanical performance of A709 in support of its code qualification.

As part of the A709 code qualification effort, this report summarizes ORNL's initial experimental findings that support the integration of A709 into the elastic-perfectly plastic (EPP) strain limits code case. It also covers thermomechanical fatigue testing conducted to develop viscoelastic material models, along with the preliminary results of creep-fatigue experiments at 816°C using the Simplified Model Test (SMT) method.

1. INTRODUCTION

Through a down-selection and an intermediate term testing program sponsored by the US Department of Energy (DOE), Office of Nuclear Energy (NE), Advanced Reactor Technologies (ART) Program, the advanced austenitic stainless steel Alloy 709 (A709) was recommended for qualification as a Class A construction material for the American Society of Mechanical Engineers (ASME) Boiler and Pressure Vessel Code, Section III, Division 5 (ASME, 2023), High Temperature Reactors. A key factor is A709's overall superior structural strength advantage over the reference Sodium Fast Reactor (SFR) construction materials (Sham, et al, 2022). A multi-laboratory materials development effort, involving the Oak Ridge National Laboratory (ORNL), the Idaho National Laboratory and the Argonne National Laboratory, was carried out to investigate the mechanical performance of A709 in support of its code qualification. The program goal is to complete the 100,000 hr Code Case data package by December 2024, finalize developing the design parameters in FY 2025, and submit the draft code case to ASME in early 2026.

This report summarizes the experiments conducted at ORNL on A709 in FY 2024, focusing on the development of elastic-perfectly plastic (EPP) and Simplified Model Test (SMT) methods. Additionally, thermomechanical fatigue testing was initiated to support the development of viscoelastic material models, and the preliminary experimental results are presented.

2. A709 MATERIALS AND SPECIMENS

The A709 materials used in this study are from the first two commercial heats of the plate product used in support of its ASME code qualification as Class A construction material in Section III, Division 5 (ASME, 2023). The A709 plates were produced by argon-oxygen-decarburization (AOD) followed by electroslag remelted (ESR). The plates were hot rolled, and solution annealed at a minimum temperature of 1150°C, conforming to ASTM A480/480M-24. An additional precipitation heat treatment (PT) of the plates was performed to ensure a balanced creep and creep-fatigue (CF) performance. The precipitation heat treatment protocol was 775°C for 10 h in air, followed by air cooling.

Table 1 summarizes the information regarding the two heats of Alloy 709 plates used in this study. The chemical compositions of the two heats of Alloy 709 with the heat numbers 58776 and 529900 are listed in Table 2. Both A709 plate materials conform to UNS 31025 and meet the chemical requirements, minimum mechanical properties and minimum grain size of No. 7 per ASTM E112 as specified in ASTM A240/A240M-24.

The specimens used for code case testing were machined at the mid-thickness for the heat 58776 plate and at the 1/4-thickness for heat 529900 plate. All specimens were along the rolling direction. In this study, the suitable test specimen used for experiments with cyclic loading, such as fatigue, creep-fatigue or thermomechanical fatigue, is the standard fatigue specimen geometry shown in Figure 1.

Table 1. A709 supply materials in plate product form

Fabricator	Master heat number	Plate ID	Nominal ASTM grain size number	Plate thickness, (in)	Material test condition
G.O. Carlson Inc	58776	58776-3RBC1	7	1.10	Precipitation treated (PT)
Allegheny Technologies Incorporated	529900	CG05368	7	1.81	
		CG05455	7		

Table 2. Chemical compositions of the A709 plates with heat number 58776 and 529900 (wt %).

Element	Heat number 58776	Heat number 529900
C	0.066	0.08
Cr	20.05	19.9
Co	0.02	0.02
Ni	25.14	24.6
Mn	0.9	0.9
Mo	1.51	1.5
N	0.152	0.15
Si	0.38	0.39
P	0.014	0.003
S	0.001	<0.001
Ti	0.01	<0.01
Nb	0.26	0.17
Al	0.02	0.02
B	0.003	0.004
Cu	0.06	0.06
Fe	balance	balance

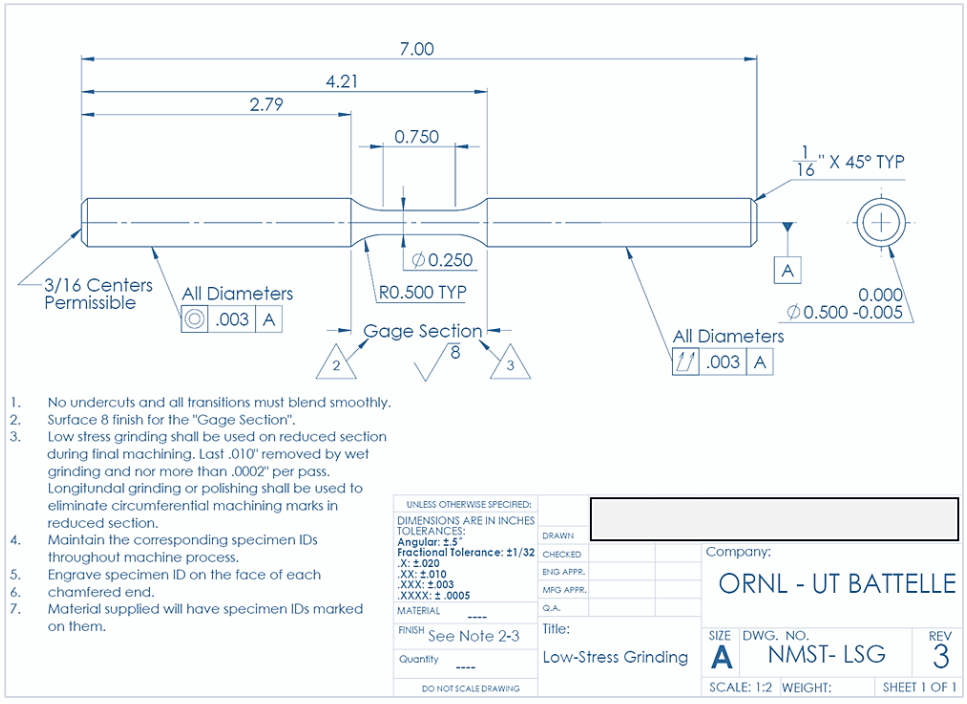

Figure 1. Standard creep-fatigue specimen geometry. Dimensions are in inches.

In parallel, a baseline creep test was performed on a standard creep frame at the stress level of 90MPa and 700 ℃ on heat 58776 specimen with PT condition. The testing procedure follows ASTM E139. The creep specimen has a nominal diameter of 0.375-in with a uniform gage length of 1.875-in, shown in Figure 2. Note that this specimen geometry complies with ASTM E139 requirement, the larger diameter than the

conventional 0.25-in was chosen specifically for long-term creep rupture testing to reduce the oxidation effect.

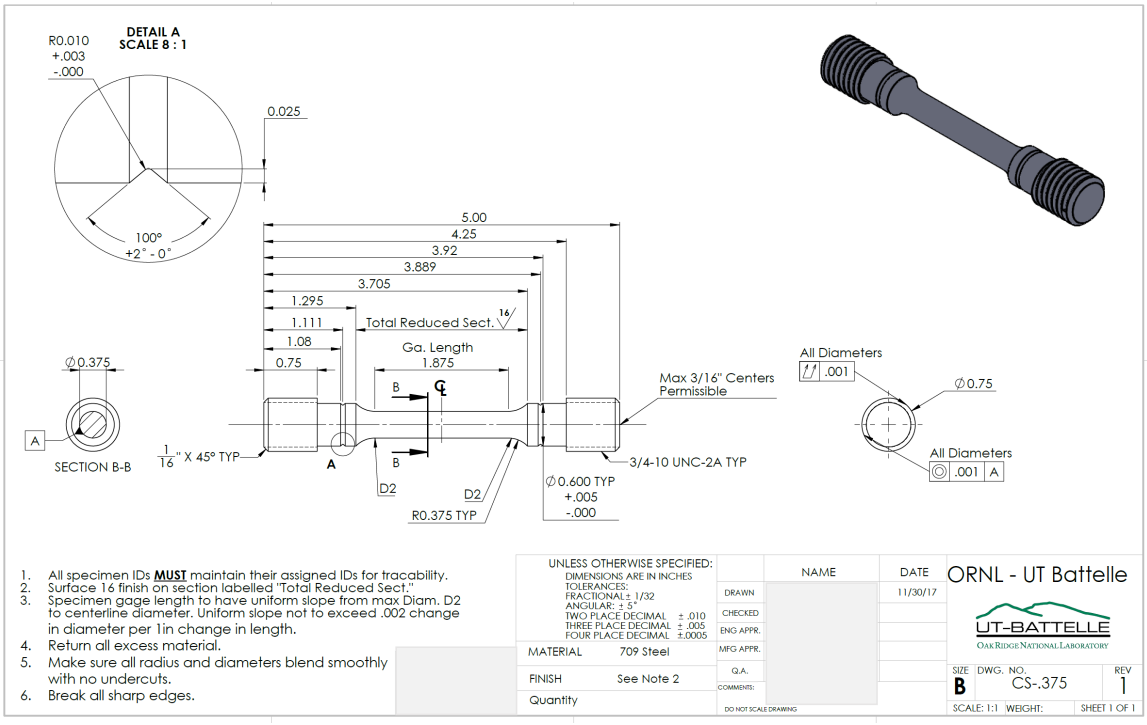

Figure 2. Creep specimen geometry. Dimensions are in inches.

3. EXPERIMENTS AND PRELIMINARY RESULTS IN SUPPORT OF EXTENSION OF THE EPP STRAIN LIMITS CODE CASE TO A709

ASME Section III Division 5 Elastic-Perfectly Plastic (EPP) code cases include N-861 for strain limits evaluation, N-862 for creep-fatigue evaluation, and N-924 for primary load limit analysis. All existing six Class A materials have been included in the EPP code cases to facilitate the use of simplified analysis methods in designing reactor components (Wang et al, 2017a, 2019a, 2021a, 2022a; Messner and Sham 2017, 2018, 2019).

These approved Class A materials for the EPP strain limits analysis are categorized as either cyclic hardening or cyclic softening. EPP analysis based on properties from unsoftened material, without any cyclic loading history, can potentially result in a lack of conservatism (Messner and Sham 2017, 2018). A specially designed experiment was performed at ORNL to support the extension of the EPP methodology to additional materials, and the evaluation method used in determining the effect of cyclic softening on the creep behavior was documented in Wang et al. (2022a) and Messner and Sham (2019).

The same experimental evaluation procedure previously developed at ORNL was adopted in this study, and the effect of prior cyclic deformation on creep properties is evaluated by introducing cyclic fatigue damage periodically into a creep test. The changes in the minimum creep rate (MCR) due to prior fatigue cycles are used to determine whether reduction factors are required to modify the isochronous stress-strain curves to account for any cyclic softening effects (Messner and Sham 2017). This study aims to

provide the initial assessment and technical basis for incorporating A709 into the EPP strain limits code case N-861.

3.1 EXPERIMENTAL APPROACH

The experimental method for evaluation of cyclic loading effect on the creep behavior is to introduce strain-controlled cyclic fatigue segments into the uniaxial creep test (Wang, et al, 2017a, 2019a, 2021a, 2022a). Figure 3 schematically illustrates the testing protocol implemented in a servo-hydraulic machine. The test starts with a load-controlled creep segment followed by unloading to zero load before switching the test machine to the strain-controlled mode and cycling for a specified number of fatigue cycles. The creep and fatigue segments are repeatedly applied to the same specimen until failure occurs. To facilitate smooth transitions between the creep segment under load-controlled mode and the fatigue segment under strain-controlled mode, the mode-switching function of the servo-hydraulic machine was utilized.

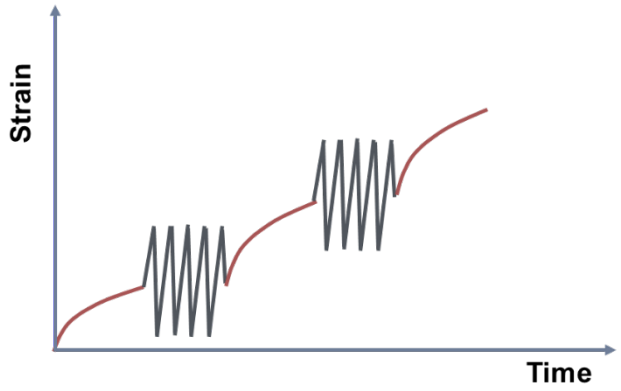

Figure 3. Schematics of the sequential creep and fatigue experiments.

Table 3 lists the detailed testing parameters on A709. The experiment was conducted at 700 ℃, a high enough temperature to ensure that the testing was in the creep region. The stress levels for the creep segment were selected to allow direct comparison with the standard uniaxial creep test at 700 ℃/90MPa. The strain-controlled fatigue segments were fully reversed with a triangle shape waveform. A strain range of 1% was selected to allow at least four fatigue segments, with 100 cycles per segment, to be applied before failure initiation in the fifth fatigue segment. The strain-controlled fatigue testing procedures are consistent with ASTM E606.

Table 3. Sequential creep and fatigue testing on A709 with heat number 58776 under PT condition.

Test temperature		700 ℃
Load-controlled creep segment	Applied stress	90 MPa
	Loading rate	1.5 s to the target stress level, equivalent to a strain rate of approximately 3E-4/s
	Creep duration	Each segment varied in duration, with each lasting a minimum of 25 hr.
Strain-controlled fatigue segment	Strain range	1%
	Strain rate	1E-3/s
	Loading ratio, *R*	-1
	Number of cycles applied in each fatigue segment	100

3.2 PRELIMINARY RESULTS ON A709

The experiment on A709 with combined sequential creep and fatigue at 700 ℃ was tested to failure. Four fatigue segments at 1% strain range were performed before fatigue failure initiation at the beginning of segment 5. The maximum and minimum stresses of all the fatigue segments are presented in Figure 4, in which the segment numbers are labeled on the maximum stress plot. The stress ranges as a function of applied cycles are for the first four segments are also presented in Figure 4. The fatigue segments showed cyclic hardening at the initial ~20 cycles and then it stabilized at the peak stresses thereafter.

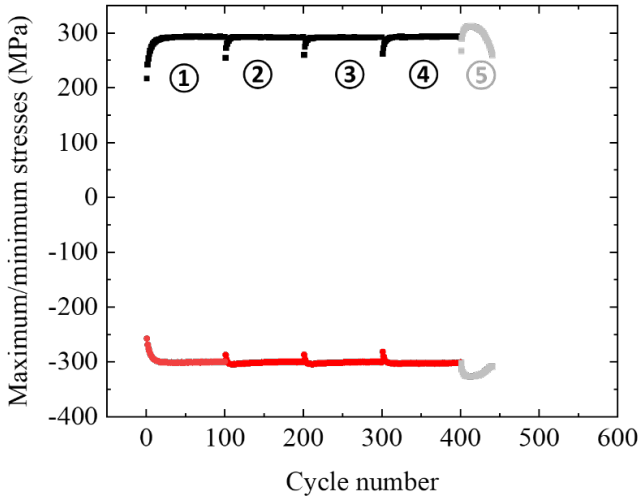

(a)

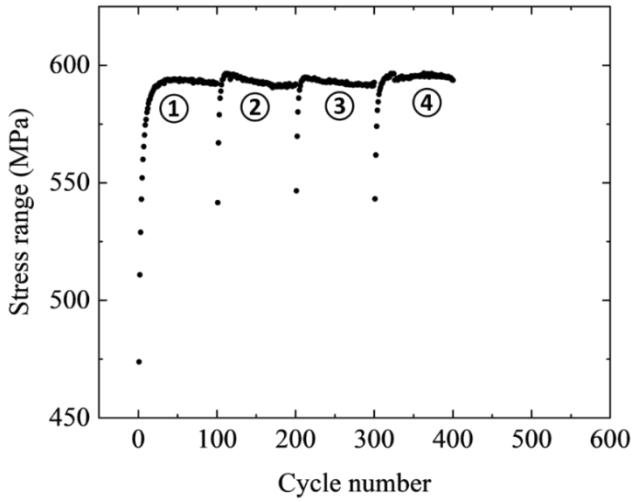

(b)

Figure 4. Maximum and minimum stresses (a) and the stress range (b) of the pure fatigue segments on A709 at 700 °C.

Prior to each fatigue segments, there was a creep segment with an applied stress of 90 MPa at the same testing temperature of 700 ºC. The creep curves of the five creep segments are plotted in Figure 5. The creep segment duration times of the first two segments were longer in order to get into the steady-state creep regime as closely as possible. The creep curve of the baseline uninterrupted standard creep test at 90 MPa and 700ºC is plotted in Figure 5 for comparison.

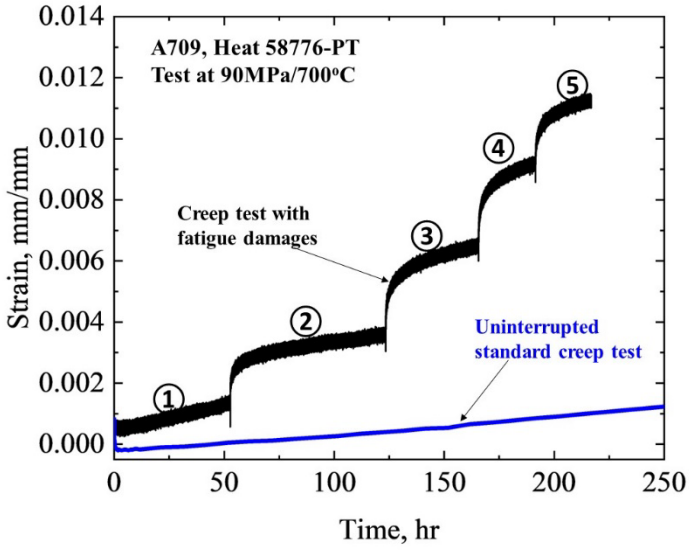

(a)

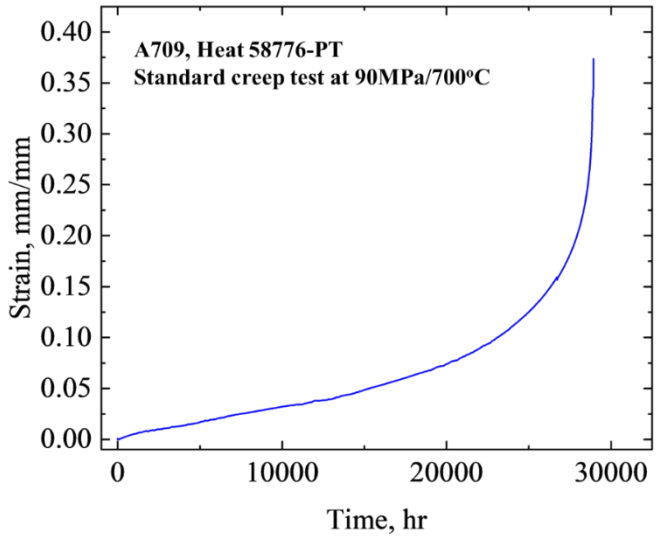

(b)

Figure 5.. Creep curves from the creep segments of the sequential creep and fatigue test (a) and the standard uninterupted creep test (b) on A709 at 700 °C and 90 MPa.

Table 4 summarizes the test durations, the accumulated creep strain at the end of the segment, and the Minimum Creep Rates (MCRs) for the sequential creep segments. The total accumulated creep time from these segments was 216.7 hr, and the total accumulated creep strain was 1.1%. With alternating creep and fatigue segments, each restart of the creep segment has led to a renewed primary creep stage, resulting in additional accumulated creep strain due to higher creep rates during this stage compared to the steady state creep stage. Therefore, it is not surprising that the test involving alternating segments accumulated a higher total creep strain than the standard uninterrupted creep test.

The uninterrupted creep test did not show an obvious transition from primary creep to the steady-state creep stage. A MCR of 4.05e-4%/h was calculated from the creep curve, and the creep rupture time was 28,929 hr with the total elongation of 39.5% and reduction of area of 79%. The much lower MCR from this test could be due to specimen-to-specimen and differences in the testing setup. The creep strain was 0.1% at a creep time of 216.7 h, which is much less than the test with alternating creep segment and fatigue segment.

Table 4. Summary of the creep segments on A709 at 90 MPa and 700 °C.

Segment no.	Prior fatigue cycles (% of fatigue damage)	Duration (h)	Accumulated creep strain (%)	MCR (%/h)
Creep 1	0/0	52.7	0.15	2.38E-3
Creep 2	100 (22%)	70.7	0.235	1.09E-3
Creep 3	200 (44%)	42.2	0.288	1.6E-3
Creep 4	300 (67%)	25.9	0.277	2.78E-3
Creep 5	400 (89%)	25.2	0.182	2.21E-3

3.3 DISCUSSIONS

These changes in the MCR are presented by normalizing the MCR measured from each creep segment with that from the first segment. Because the first segment did not have any prior cyclic deformation, it represents the behavior of a standard creep test. The normalized MCRs of the creep segments for A709 at 700°C/90 MPa are plotted in Figure 6. For comparison, the results for Grade 91 at three test conditions—600 °C/150 MPa, 625 °C/130 MPa, and 650 °C/99 MPa, 2.25Cr-1Mo at 650 °C/42 MPa and Alloy 800H at 750 °C/55 MPa are also presented in the same figure (Wang et al. 2022a). With ~90% of the fatigue damage, negligible changes in the MCR were observed. The introduction of significant fatigue damage to the A709 material does not appear to significantly alter its creep behavior. Therefore, it is not recommended to incorporate any softening factor for A709 in the EPP analysis, though further testing is needed to validate this recommendation.

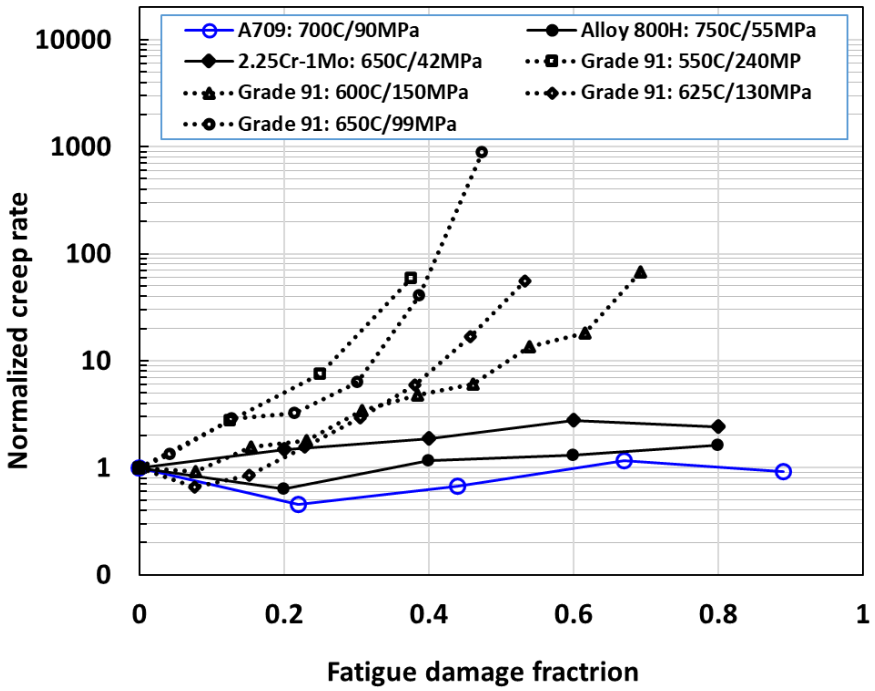

Figure 6. Effect of fatigue damage on the MCRs of A709, Alloy 800H, 2.25Cr-1Mo, and Grade 91.

4. THERMOMECHANIAL TESTING IN SUPPORT OF THE DEVELOPMETN OF A VISCOPLASTIC MODEL FOR A709

Thermomechanical testing was conducted on A709 to generate data for assessing its temperature-dependent responses to cyclic thermomechanical loading. The data generated can be used to verify design criteria for components and, importantly, to aid in the development and validation of viscoplastic material models. The experimental data provided crucial information for calibrating temperature-dependent parameters of the material models.

A series of thermomechanical fatigue experiments are planned, including various temperature ranges and both in-phase and anti-phase loading configurations. The initial experimental results on A709 with heat number 529900 under PT condition are summarized in this report.

4.1 THERMOMECHANICAL TESTING METHOD

The thermomechanical fatigue experiment was performed at a temperature range of 350 to 950^{o} C with heating and cooling rates of 30^{o} C/min using an igniter heater furnace. The temperature profile was automated and controlled by a LabView program. The thermomechanical fatigue was conducted following the ASTM-2368 standard. The test was under strain control with straining cycles that are 180 degrees out-of-phase with the thermal cycles. The total strain was controlled to be zero and the starting temperature was 650^{o} C, the mid-point of the thermal cycle. The applied strain ratio is -1. The testing parameters are listed in Table 5.

Table 5. Thermomechanical fatigue testing on A709 with heat number 529900

Test temperature range	350° C to 950° C
Specimen diameter, inch	0.25
Controlled total strain amplitude	Zero
Starting temperature	650° C
Heating and cooling rates	30° C/min
Strain ratio	-1
Temperature mechanical strain phase angle	180 °, i.e., anti-phase thermomechanical fatigue
Experiment control mode	Strain control

4.2 PRELIMINARY RESULTS ON A709

The mechanical strain is calculated by subtracting the thermal expansion from the total strain. The thermal expansion coefficient (CTE) of A709 was measured by Smith et al (2017) to 850 °C, and the values are reported to be 16.9E-6 mm/mm/ °C at 350 °C and 18.2E-6 mm/mm/ °C at 850 °C. A simple linear relationship was assumed between the CTE and testing temperature in this analysis, and CTE values are extrapolated to 950 °C using this linear extrapolation. The strain range for this test was 1.17%. The strain rate was determined by the heating and cooling rate, and it was 9.3E-6 s^{-1}.

The experiment is ongoing at the time of writing this report, and it is planned to test this specimen to failure. The experimentally measured thermal cycle and mechanical strain history in one thermal cycle are plotted in Figure 7. The representative hysteresis loops, and the maximum and minimum stresses from the available cycles are plotted in Figure 8. The maximum stress values are higher than the minimum stresses due to tensile stress being the material's response during cooling to 350°C in the cycle, whereas compressive stress occurred during heating to the highest temperature of 950°C. The cyclic hardening effect is evidently shown from the hysteresis loops and the maximum and minimum stresses.

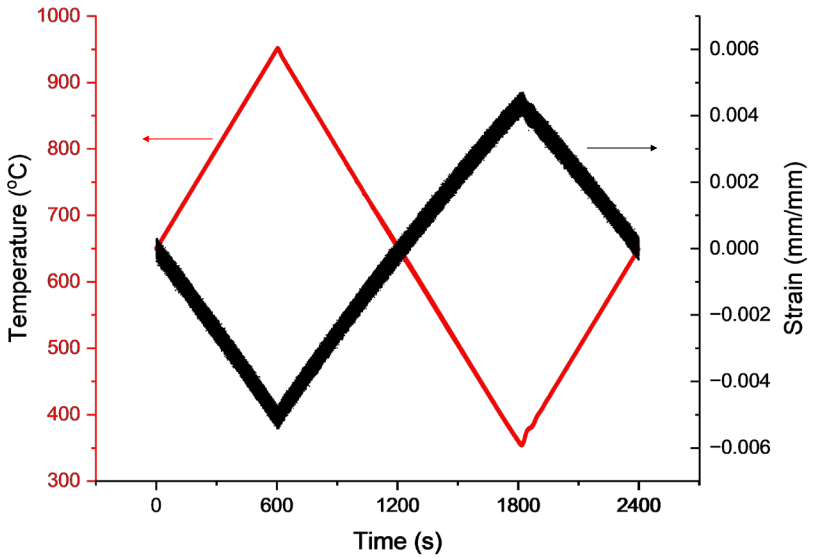

Figure 7.. Temperature and mechancial strain history of one thermal cycle.

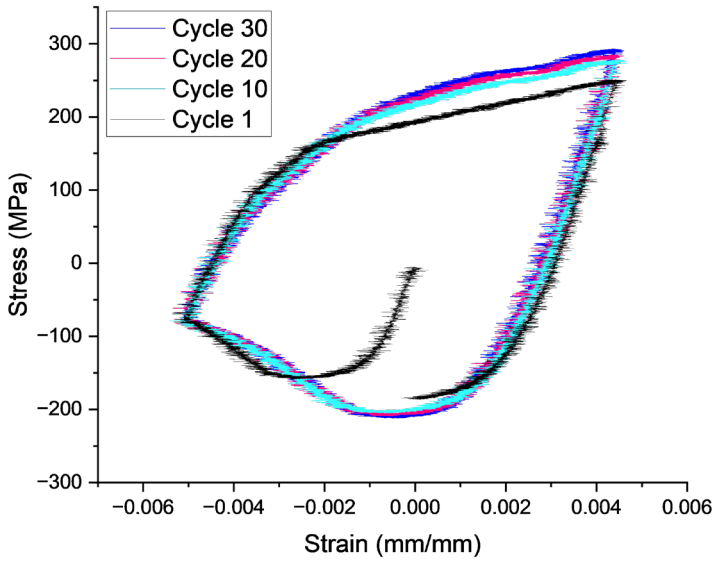

(a)

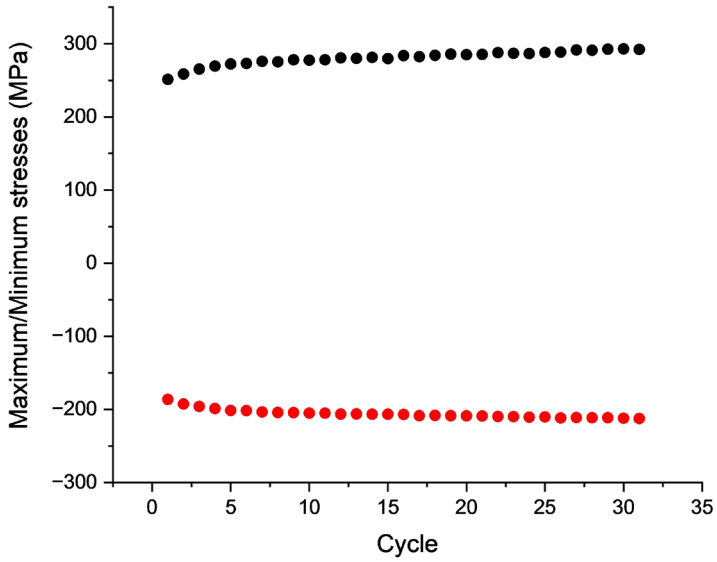

(b)

Figure 8. Thermomechanical fatigue on A709 at temperature range of 350 to 950° C with representative hysteresis loops (a) and maximum and minimum stresses (b).

5. SMT EXPERIMENTS IN SUPPORT OF EPP AND SMT DESIGN METHODS FOR A709

5.1 INTEGRATED EPP AND SMT CREEP-FATIGUE EVALUATION

For high temperature components under cyclic loading, creep-fatigue (CF) is the most dominating structural failure mode. In the last 40 years, significant efforts have been devoted to elevated temperature

code rule development in the ASME Section III, Division 5, Subsection HB, Subpart B to ascertain conservative structural designs against CF failure. The current CF evaluation in the design procedure is based on the CF interaction damage diagram, where the evaluation procedure separately calculates the creep damage using the stress quantity and the fatigue damage through the strain quantity before recombining the results to obtain a damage sum. The deconstruction of the stress and strain and recombination of the damage quantities present difficulties in evaluation of the test data and determination of cyclic damage in design, and the uncertainties in these steps lead to the use of overly conservative design factors in the current CF evaluation procedure.

Recently, there have been major developments in an alternative CF evaluation concept based on an integrated EPP and Simplified Model Test (SMT) approach. The approach avoids separate evaluation of creep and fatigue damage, eliminates the requirement for stress classification, and greatly simplifies the evaluation of elevated temperature cyclic service (Jetter, 1998; Wang et al., 2013, 2014, 2015, 2017b, 2019b, 2019c, 2021b, Hou et al, 2022). This integrated EPP and SMT methodology aims to minimize the over-conservatism in the existing CF evaluation procedure using the damage interaction diagram, while properly accounting for localized defects and stress risers. The SMT based experimental data accounts for the stress and strain redistribution, representing a real phenomenon in structure component under high temperature cyclic loading where enhanced creep damage occurs. This stress and strain redistribution are characterized as the elastic follow up effect. Referring to Figure 9, elastic follow-up may be quantified by computing the ratio of ε_{0-2}, the creep strain in the test section including elastic follow-up, to the creep strain that would have occurred under pure relaxation, ε_{0-1}. Thus, the elastic follow-up, Q, is given by:

$$Q = (\varepsilon_{0-2})/(\varepsilon_{0-1}) \tag{1}$$

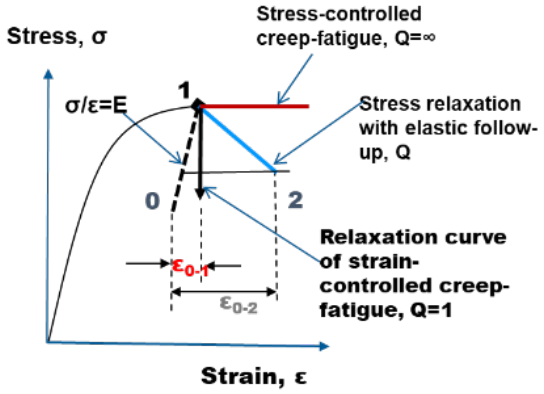

Figure 9. Definition of elastic follow-up

Elastic follow-up can cause larger strains in a structure with displacement-controlled loading than would be predicted using an elastic analysis. Wang et al. (2015, 2017b, 2019c) advanced SMT experimental techniques in the recent years, particularly with the newly developed single-bar SMT (SBSMT) test method and protocol (Wang et al, 2019c). The SBSMT test method greatly simplifies the procedure of generating SMT test data and accelerates the development of SMT-based design methods. These innovations successfully addressed numerous challenges encountered in SMT key feature experiments, allowing for the evaluation of elastic follow-up effects using a standard CF specimen, without requiring specialized instrumentation or specimen design.

5.2 SMT TEST RESULTS ON A709 AT 816 ^{O}C

Experiments in developing the integrated EPP and SMT method for A709 were initiated in FY 2024, and the preliminary results are summarized in this report. This test on A709 at 816 ºC was conducted using the SBSMT test method on a standard fatigue specimen shown in Figure 1. The hold time was 1800sec, applied to the peak tensile amplitude. The test specimen was machined from heat 529900, plate CG05455, with PT condition.

As shown in the representative measured hysteresis loops presented in Figure 10, the test specimen continued to accumulate creep strain during the relaxation process after initial loading, illustrated by the sloped relaxation indicated with the green dashed line. The elastic follow-up factor for this test was calculated to be 3.4, using an elastic modulus value of 145 GPa (Reese et al., 2021). The stress relaxation history of the initial three cycles is presented in Figure 10b.

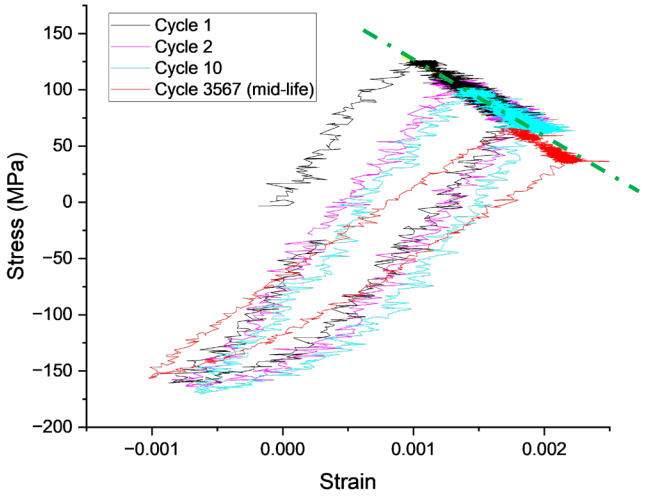

(a)

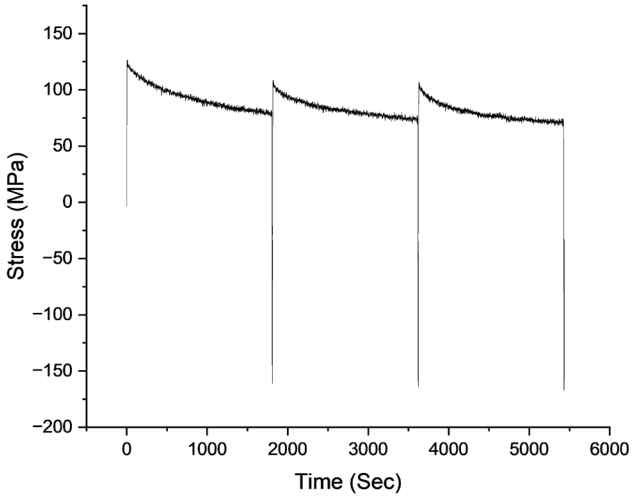

(b)

Figure 10. Hysteresis loops (a) and stress history of the initial three cycles (b) of the SBSMT on A709 at 816 ºC with an elastic follow up factor of 3.4.

The maximum and minimum stresses and the strain range as a function of applied cycles are plotted in Figure 11. There was an initial stage for about 700 cycles where the peak stresses decreased while the strain ranges increased rapidly, before entering to a steady state. The mean strain range of this test is 0.34%, in the low strain range region. The specimen was tested until failure occurred after 7134 cycles, spanning a total test duration of close to 3600 hours, a long test duration for strain-controlled CF experiments.

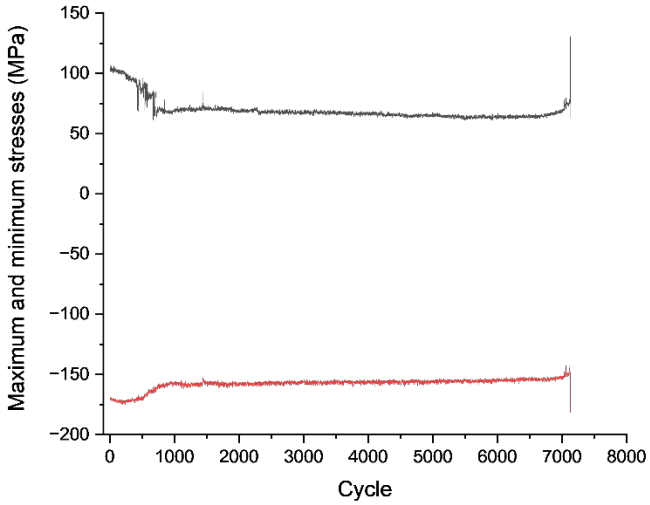

(a)

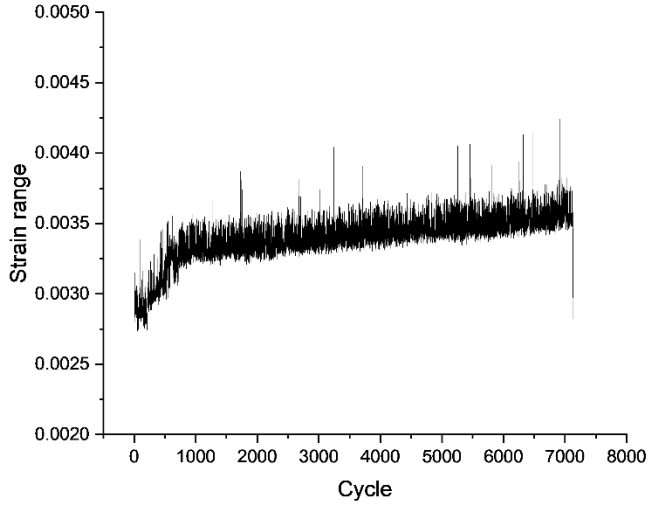

(b)

Figure 11. Maximum and minimum stresses (a) and strain range (b) of the SBSMT on A709 at 816 ºC with an elastic follow up factor of 3.4.

6. SUMMARY

Experiments were conducted on A709 to support its integration into ASME EPP strain limit analysis. The results indicate that prior cyclic deformation has an insignificant effect on its creep behavior. Therefore, reduction factors on the isochronous stress-strain curves are not recommended when incorporating A709 into EPP analysis, though additional tests are advised to confirm this finding.

Thermomechanical testing was initiated on A709 to gather data for evaluating its temperature-dependent responses in developing viscoplastic material models. Additionally, the SBSMT method was applied to design experiments for A709 with an elastic follow-up factor of 3.4 at low strain ranges, and long test duration SMT creep-fatigue failure data was successfully generated.

REFERENCES

ASME (2023). Boiler and Pressure Vessel Code, Section III Division 5, *Rules for Construction of Nuclear Facility Components,* Subsection HB Subpart B, American Society of Mechanical Engineers, New York, NY.

ASME B&PV Code Case N-861, *Satisfaction of Strain Limits for Division 5 Class A Components at Elevated Temperature Service Using Elastic-Perfectly Plastic Analysis*, ASME Section III Division 5.

ASME B&PV Code Case N-862, *Calculation of Creep-Fatigue for Division 5 Class A Components at Elevated Temperature Service Using Elastic-Perfectly Plastic Analysis,* ASME Section III Division 5.

ASME B&PV Code Case N-924, *Design Rules and Limits for Load-Controlled Stresses for Class A Components at Elevated Temperature Service Using Elastic-Perfectly Plastic and Simplified Inelastic Analyses,* ASME Section III Division 5.

ASTM E139-11 (2018), *Standard Test Methods for Conducting Creep, Creep-Rupture, and Stress-Rupture Tests of Metallic Materials*, ASTM International, West Conshohocken, PA, 2011, www.astm.org

ASTM E606 / E606M-21, *Standard Test Method for Strain-Controlled Fatigue Testing*, ASTM International, West Conshohocken, PA, 2021, www.astm.org

ASTM A480/480M-24 (2024), *Standard Specification for General Requirements for Flat-Rolled Stainless and Heat-Resisting Steel Plate, Sheet, and Strip,* ASTM International, West Conshohocken, PA, 2020, www.astm.org

ASTM A240/A240M-24 (2024), *Standard Specification for Chromium and Chromium-Nickel Stainless Steel Plate, Sheet, and Strip for Pressure Vessels and for General Applications,* ASTM International, West Conshohocken, PA, 2020, www.astm.org

ASTM E112 (2021), *Standard Test Methods for Determining Average Grain Size,* ASTM International, West Conshohocken, PA, 2020, www.astm.org

ASTM-2368-10 (2017), *Standard Practice for Strain Controlled Thermomechanical Fatigue Testing,* ASTM International, West Conshohocken, PA, 2020, www.astm.org

Jetter, R.I., *(1998), An Alternate Approach to Evaluation of Creep-Fatigue Damage for High Temperature Structural Design Criteria, Fatigue, Fracture, and High Temperature Design Methods in Pressure Vessels and Piping,* Book No. H01146 -1998, PVP365, 199-206.

S.J. Reese, D.S. Smith, R.E. Rupp, J.K. Wright, A.R. Khanolkar, R.N. Wright, and D.H. Hurley (2021), *Elevated-Temperature Elastic Properties of Alloys 709 and 617 Measured by Laser Ultrasound*, JMEPEG (2021) 30:1513–1520.

D.S. Smith, N.J. Lybeck, J.K. Wright, R.N. Wright (2017), *Thermophysical properties of Alloy 709*, Nuclear Engineering and Design 322 (2017) 331–335

Messner, M. C. and Sham, T.-L., (2017), *FY17 Status Report on the Initial EPP Finite Element Analysis of Grade 91 Steel*, Technical Report No. ANL-ART-94, Argonne National Laboratory, Chicago, IL.

Messner, M. C. and Sham, T.-L. (2018), *Initial development and extension of EPP methods to Grade 91,* ANL-ART-133, Argonne National Laboratory, Chicago, IL.

Messner, M. C. and Sham, T.-L. (2019), *Draft ASME Section III Division 5 Code Cases to extend EPP strain limits and creep-fatigue design methods to Grade 91*, ANL-ART-165, Argonne National Laboratory, Chicago, IL.

Sham, T.-L., Wang, Y., Bass, R., and Zhang, X. (2022), *A709 Qualification Plan Update and Mechanical Properties Data Assessment, INL/RPT-22-67641*, Idaho National Laboratory, Idaho Falls, ID.

Wang, Y., Messner. M. C., and Sham, T.-L. (2017a). *FY17 Status Report on Testing Supporting the Inclusion of Grade 91 Steel as an Acceptable Material for Application of the EPP Methodology,* ORNL/TM-2017/388. Oak Ridge, TN: Oak Ridge National Laboratory.

Wang, Y., Jetter, R. I., Messner, M. C. and Sham, T.-L. (2019a), *Report on FY19 Testing in Support of Grade 91 Core Block Code Case,* ORNL/TM-2019/1280, Oak Ridge National Laboratory, Oak Ridge, TN.

Wang, Y., Hou, P., and Sham, T.-L.(2021a), *Report on FY 2021 Testing in Support of Integrating Alloy 800H and 2.25Cr-1Mo for EPP Analysis,* ORNL/TM-2021/2189, Oak Ridge National Laboratory, Oak Ridge, TN.

Wang, Y., Hou, P., and Sham, T.-L.(2022a), *Experimental Basis for the Extension of Elastic Perfectly Plastic Strain Limits Evaluation Procedure of ASME Section III, Division 5 Code Case N 861 to Grade 91, Alloy 800H And 2.25Cr-1Mo,* PVP2022-84817, Proceedings of the ASME 2022 Pressure Vessels and Piping Conference, PVP2022-84817, American Society of Mechanical Engineers, New York, NY.

Wang, Y., Jetter, R. I., Krishnan, K., and Sham, T.-L (2013), *Progress Report on Creep-Fatigue Design Method Development Based on SMT Approach for Alloy 617*, ORNL/TM-2013/349, Oak Ridge National Laboratory, Oak Ridge, TN.

Wang, Y., Jetter, R. I. and Sham, T.-L (2014), *Application of Combined Sustained and Cyclic Loading Test Results to Alloy 617 Elevated Temperature Design Criteria*, ORNL/TM-2014/294, Oak Ridge National Laboratory, Oak Ridge, TN.

Wang, Y., Sham, T.-L, and Jetter, R. I., (2015), *Alloy 617 Creep–Fatigue Damage Evaluation Using Specimens with Strain Redistribution*, Journal of Pressure Vessel Technology, 137 (3), 021402

Wang, Y., Jetter, and Sham, T.-L. (2017b), *Pressurized Creep-Fatigue Testing of Alloy 617 Using Simplified Model Test Method*, Proceedings of the ASME 2017 Pressure Vessels and Piping Conference, PVP2017-65457, American Society of Mechanical Engineers, New York, NY.

Wang, Y., Jetter, R. I., and Sham, T.-L. (2019b), *Effect of Internal Pressure on the Creep-fatigue Performance of Alloy 617 Based on Simplified Model Test Method*, Proceedings of the ASME 2019 Pressure Vessels and Piping Conference, PVP2019-93650, American Society of Mechanical Engineers, New York, NY.

Wang, Y., Jetter, R. I., Messner, M., and Sham, T.-L. (2019c), *Development of Simplified Model Test Method for Creep-fatigue Evaluation*, Proceedings of the ASME 2019 Pressure Vessels and Piping Conference, PVP2019-93648, American Society of Mechanical Engineers, New York, NY.

Wang, Y., Hou, P., Jetter, R. I., & Sham, T. L. (2021b). *Evaluation of Primary-Load Effects on Creep-Fatigue Life of Alloy 617 Using Simplified Model Test Method*. Proceedings of the ASME 2021 Pressure Vessels and Piping Conference, PVP2021-61658, American Society of Mechanical Engineers, New York, NY.

Hou, P., Jetter, R. I., & Sham, T. L (2022), *An Experimental and Analytical Study on the Development of Extrapolation Method for the Creep-Fatigue Life of Alloy 617 to Low Strain Ranges and Long Hold Times at 950°C,* Proceedings of the ASME 2022 Pressure Vessels and Piping Conference, PVP2022-84783, American Society of Mechanical Engineers, New York, NY.